***JKPK (JURNAL KIMIA DAN PENDIDIKAN KIMIA)**, Vol. 9, No.2, 2024* *pp. 298-310*
Chemistry Education Study Program, Universitas Sebelas Maret *ISSN 2503-4146*
https://jurnal.uns.ac.id/jkpk *ISSN 2503-4154 (online)*

SYNTHESIS AND CHARACTERIZATION POLYANILINE/CuO NANOCOMPOSITES WITH VARIOUS TEMPERATURE

Risa Rahmawati Sunarya[1*], Yosi Yosiva Sidik[1], Fitri Nur Islamiati[2]

[1]Department of Chemistry Education, Faculty of Tarbiyah and Teacher Training, UIN Sunan Gunung Djati, Bandung, Indonesia
[2]Department of Chemistry, Ulsan National Institute of Science and Technology, Ulsan, Republic of Korea

ARTICLE INFO

Keywords:
polyaniline;
polyaniline/CuO nanocomposites;

Article History:
Received: 2024-07-20
Accepted: 2024-08-21
Published: 2024-08-30
*d*oi:10.20961/jkpk.v9i2.90819

ABSTRACT

Polyaniline (PANI) metal oxide composites are known for their high electrical conductivity, environmental stability, and enhanced mechanical strength, making them valuable in applications such as sensors, batteries, and electromagnetic shielding. This study synthesises and characterises PANI/CuO nanocomposites to examine their structural, morphological, and functional properties at different synthesis temperatures. The material's capabilities are significantly enhanced by integrating the conductive polymer PANI with copper oxide (CuO), a p-type semiconductor with a narrow band gap. The oxidative polymerization of aniline, the process by which PANI is formed, requires precise control of oxidizing agents and reaction conditions, as these factors directly affect the polymerization, conductivity, and overall properties of the resulting nanocomposite. The PANI/CuO nanocomposites were synthesized at three different temperatures: 10℃, 25℃, and 50℃, to determine how temperature affects their characteristics. Fourier Transform Infrared (FTIR) spectroscopy and Scanning Electron Microscopy (SEM) were employed to analyze these nanocomposites. FTIR results revealed shifts in the quinoid and benzenoid rings, indicating hydrogen bonding between the NH group of PANI and the CuO surface, which accelerates charge transfer. The SEM analysis showed that while pure PANI exhibits a uniform globular morphology, the PANI/CuO nanocomposites display a nanorod morphology. These morphological differences impact the surface area and electrical conductivity of the composites, highlighting the significance of temperature in tailoring the material's properties for specific applications.

**Corresponding Author Email:* risarahmawatis@uinsgd.ac.id
How to cite: R. R. Sunarya, Y. Y. Sidik, and F. N. Islamiati**,** "Synthesis and characterization of polyaniline/CuO nanocomposites with various temperature," *Jurnal Kimia dan Pendidikan Kimia (JKPK)*, vol. 9, no. 2, pp. 298-310, 2024. Available: http://dx.doi.org/10.20961/jkpk.v9i2.87294.

INTRODUCTION

Composites formed by combining conductive polymers with metal oxide nanoparticles have become a significant focus in advanced materials research due to their synergistic properties [1-8]. The size, morphology, and conductive properties of polymers are greatly influenced by the incorporation of metal oxides such as graphene oxide [9-13], CuO [6-7, 14-17], SiO_2 [18], ZnO [5], TiO_2 [2], and V_2O_5 [19, 20]. These metal oxides enhance the conductivity and thermal stability of the composites, making them valuable for a wide range of applications.

Polyaniline (PANI), a conductive polymer, has been extensively studied due to its remarkable electrical conductivity, environmental durability, and ease of synthesis [1, 6, 8-10, 12, 21-25]. PANI-metal oxide composites exhibit unique properties such as high electrical conductivity, environmental stability, and enhanced mechanical strength, making them highly desirable for global applications. These composites show significant potential in industries such as energy storage, where they can improve battery performance, environmental sustainability through advanced sensors for pollution detection, and electronics by providing effective electromagnetic shielding [1, 17, 22, 26].

PANI has been synthesized at various temperatures, leading to composites with different properties. Research indicates that PANI synthesized at lower temperatures exhibits the highest conductivity [25]. This conductivity is attributed to the π-conjugated backbone of PANI, which facilitates charge mobility between the polymer and the matrix [9, 11, 12, 21, 23, 25].

The addition of metal oxide nanoparticles to PANI enables easy modification of these composites, making them promising candidates for applications in sensing, electronics, and energy storage [1, 17, 22, 26]. Specifically, incorporating CuO into PANI improves the composite's electrical conductivity and thermal stability [6, 7]. To achieve a well-defined and optimised material structure, PANI-based metal oxide composites are synthesised and characterised using multi-step approaches, such as the rapid mixing method [25] and electrochemical methods [10]. Careful selection of metal oxides, combined with the unique properties of PANI, enhances conductivity, stability, and reactivity [1, 7, 14-17, 22, 26, 27, 28-32].

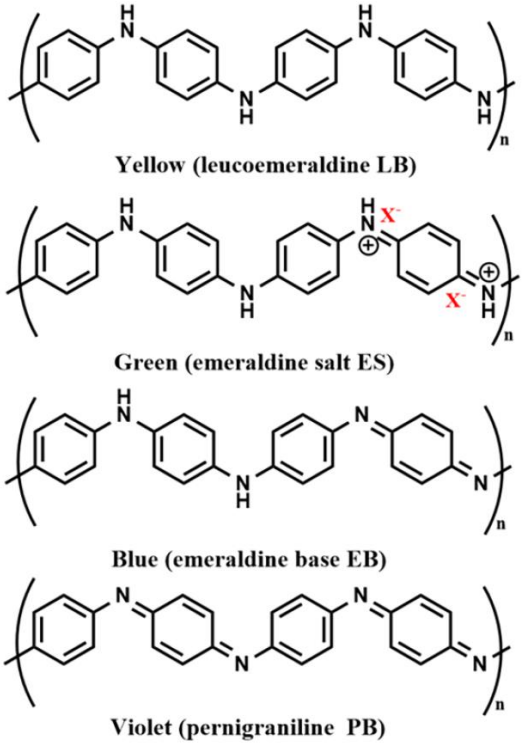

Figure 1. PANI structures based on redox states [23].

PANI is produced through the oxidation of aniline, resulting in various forms depending on the degree of oxidation [23, 25]. The partially oxidised form is emeraldine, while the fully oxidised form is pernigraniline. These forms transform upon doping into emeraldine salts, the most conductive forms of PANI. The unique structure of PANI, which allows for multiple oxidation states, significantly impacts its performance and conductivity [23, 25]. PANI is also recognised as a multi-colour electrochromic material, displaying various colours depending on its oxidation state, as illustrated in Figure 1. These states include the yellow-colored

leucoemeraldine base (LB), the green-colored emeraldine salt (ES), the blue-colored emeraldine base (EB), and the violet-colored pernigraniline base (PB). The emeraldine salt is the most conductive form, making it highly valuable in various applications [23, 25].

While PANI/CuO nanocomposites have been extensively studied for their enhanced electrical and thermal properties, the influence of synthesis temperature on the structural and functional characteristics of these composites still needs to be explored. This study uniquely contributes to the field by systematically investigating the impact of temperature variations—specifically at 10℃, 25℃, and 50℃—on the synthesis and characterisation of PANI/CuO nanocomposites. By analysing how different temperatures affect these composites' morphology, crystallinity, and conductivity, this research offers new insights into optimising material properties for specific applications. The novel approach of correlating temperature with material performance sets this work apart from existing studies and paves the way for the tailored design of PANI/CuO nanocomposites in advanced technological applications.

Recently, PANI has garnered significant interest for its ability to form stable composites with inorganic particles. The addition of CuO, in particular, has been studied to examine the core-shell structure of PANI and enhance its thermal stability [17]. However, despite these advancements, more comprehensive studies that systematically explore the influence of synthesis methods and conditions on the structural and functional properties of PANI/CuO nanocomposites across various temperatures need to be conducted. Understanding the interaction between CuO and PANI at different temperatures is crucial for gaining theoretical insights and practical applications.

METHODS

1. Materials

The materials used in this study included ammonium persulfate (Merck, analytical grade), aniline (Merck, analytical grade), hydrochloric acid (Merck, >37%), CuO (Merck, analytical grade), and acetone (technical grade).

2. Equipment

The equipment used consisted of glassware, Whatman filter paper No. 41, a magnetic stirrer, a Fourier transform infrared (FTIR) spectrophotometer (Shimadzu Prestige-21), and a scanning electron microscope (SEM) (JEOL JSM 6510-LA).

3. Preparation of Pure PANI

Polyaniline (PANI) in the form of emeraldine salt was synthesised using a conventional polymerisation method through chemical oxidation under acidic conditions. First, 11.42 g of ammonium persulfate was dissolved in 100 mL of distilled water in one flask. Separately, 3.64 g of aniline was mixed with 100 mL of 1 M hydrochloric acid in another flask. Both flasks were placed in an ethylene glycol bath at 0°C for 1 hour.

The ammonium persulfate solution was added dropwise to the aniline solution while stirring at 700 rpm. The reaction mixture was

stirred continuously for 24 hours at 0°C. The schematic of pure PANI synthesis is shown in Figure 2. After the reaction, the green precipitate formed was separated by filtration using ashless slow filter paper (Whatman No. 41). The precipitate was thoroughly washed with acetone and hydrochloric acid solution until the washing liquid became colourless [11].

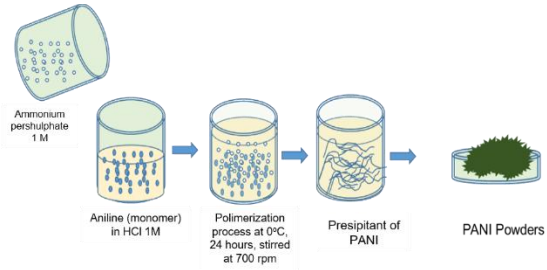

Figure 2. Schematic of pure PANI synthesis

4. Preparation of PANI/CuO Nanocomposites at 10°C

To synthesize PANI/CuO nanocomposites at ten °C, 3.64 g of aniline and 2 g of CuO were mixed and stirred at 700 rpm at room temperature. Then, 100 mL of 1 M HCl solution was slowly added to the aniline/CuO mixture. This mixture was then stirred at 700 rpm for 4 hours at 10°C. Separately, 11.42 g of ammonium persulfate was dissolved in 100 mL of distilled water and stirred until the solution was homogeneous. The ammonium persulfate solution was added dropwise to the aniline/CuO-doped HCl solution. The mixture was stirred continuously at 700 rpm for 24 hours at 10°C.

Using the interface method, this polymerisation process results in the formation of PANI/CuO nanocomposites. The synthesis schematic is shown in Figure 3. The mixture was filtered using Whatman No. 41 filter paper and washed with 1 M HCl and acetone solution until the filtrate became colourless. The filtered solid was then placed on a baking sheet, covered with aluminium foil with small holes, and oven-dried at 50°C for 5 hours. The dried PANI/CuO nanocomposites were finely ground using a mortar and pestle to obtain the final product.

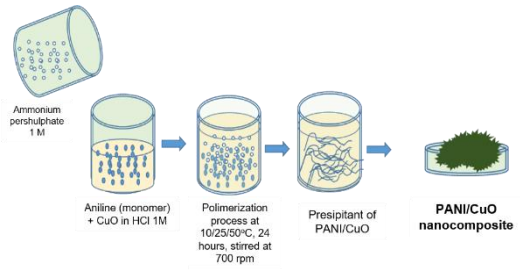

Figure 3. Schematic of PANI/CuO nanocomposites synthesis.

5. Preparation of PANI/CuO Nanocomposites at 25°C and 50°C

The same procedure was used for synthesizing PANI/CuO nanocomposites at 10°C, followed by synthesis at 25°C and 50 °C. These temperatures were selected to investigate the effect of temperature on the conductivity and morphology of the nanocomposites [25].

6. Characterization

The synthesised PANI and PANI/CuO nanocomposites were characterised using Fourier Transform Infrared (FTIR) spectroscopy and Scanning Electron Microscopy (SEM). FTIR analysis was performed using a Shimadzu Prestige-21 spectrophotometer over the wavenumber range of 400–3500 cm^{-1} to identify functional groups and confirm the successful synthesis of the composites. For SEM analysis, the surface morphology of the PANI/CuO nanocomposites was examined using a JEOL JSM 6510-LA scanning electron microscope. The samples were sputter-

coated with a thin layer of gold to enhance conductivity and imaging quality, and SEM imaging was conducted at an acceleration voltage of 15 kV.

RESULTS AND DISCUSSION

1. Synthesis of PANI and PANI/CuO Nanocomposites

Polyaniline (PANI) is a conductive polymer that can be synthesised efficiently and cost-effectively. This study synthesised PANI in its emeraldine salt (ES) form through polymerisation using rapid mixing. In this process, an ammonium persulfate (APS) oxidiser solution ($(NH_4)_2S_2O_8$) was gradually added dropwise into an aniline solution. The polymerisation was conducted at a temperature of 0°C for 24 hours.

The rapid mixing method offers several advantages over electro-polymerization and interfacial polymerisation methods. It is a simple and inexpensive process that can be easily scaled up for large-scale production. Using low temperatures and acidic conditions is crucial to ensuring that the polymerisation mechanism follows an electron acceptor pathway facilitated by the oxidant. In contrast, polymerisation at higher temperatures and under primary conditions can lead to the homolytic cleavage of peroxide bonds, forming radical species containing oxygen. This shift alters the mechanism to an oxygen donor pathway.

The chemical reaction for forming PANI-ES using APS as an oxidiser in an HCl solution is illustrated in Figure 4.

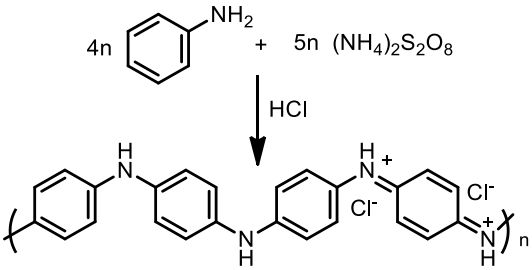

Figure 4. PANI-ES formation reaction.

PANI in the form of emeraldine salt is a dark greenish powder; Figure 5 shows PANI after filtration before the drying process.

Figure 5. PANI after the filtration process.

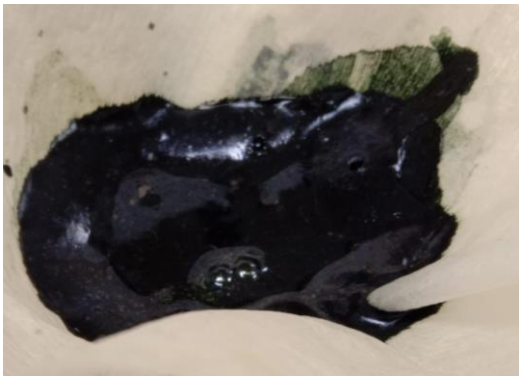

Figure 6. PANI/CuO nanocomposite after filtration.

The PANI/CuO nanocomposites were synthesised following the same procedure used for pure PANI synthesis, with the primary difference being the addition of CuO powder to the aniline monomer before the polymerisation process. The incorporation of CuO into the aniline is intended to enhance

the properties of the composite, particularly by increasing the electrical conductivity and thermal stability of the PANI/CuO nanocomposite [17]. The formation of PANI/CuO nanocomposites is facilitated by hydrogen bonds between the PANI and CuO on the CuO surface [17]. As shown in Figure 6, the resulting PANI/CuO nanocomposite after filtration has a darker greenish colour compared to pure PANI, indicating the successful incorporation of CuO.

2. Analysis of FTIR Spectrum of PANI/CuO Nanocomposites

The PANI/CuO nanocomposites were characterised using FTIR spectroscopy and SEM. The FTIR spectra of pure PANI and PANI/CuO nanocomposites were recorded in the 400–2100 cm^{-1} wavelength range, as shown in Figure 7. For pure PANI, key absorption peaks were observed at 1237 cm^{-1} and 1292 cm^{-1}, corresponding to C–H stretching from aromatic conjugation and C–N stretching from the secondary aromatic amine, respectively. Additionally, the peak at 798 cm^{-1} was attributed to the 1,4-disubstituted benzene ring, and the peak at 1124 cm^{-1} was associated with B–NH^{+}=Q stretching, which is characteristic of conductive PANI, often referred to as the "electronic-like absorption peak" [9, 11, 25]. The peaks at 1489 cm^{-1} and 1555 cm^{-1} correspond to the stretching vibrations of the benzenoid (B) and quinoid (Q) rings, respectively [11, 17, 25].

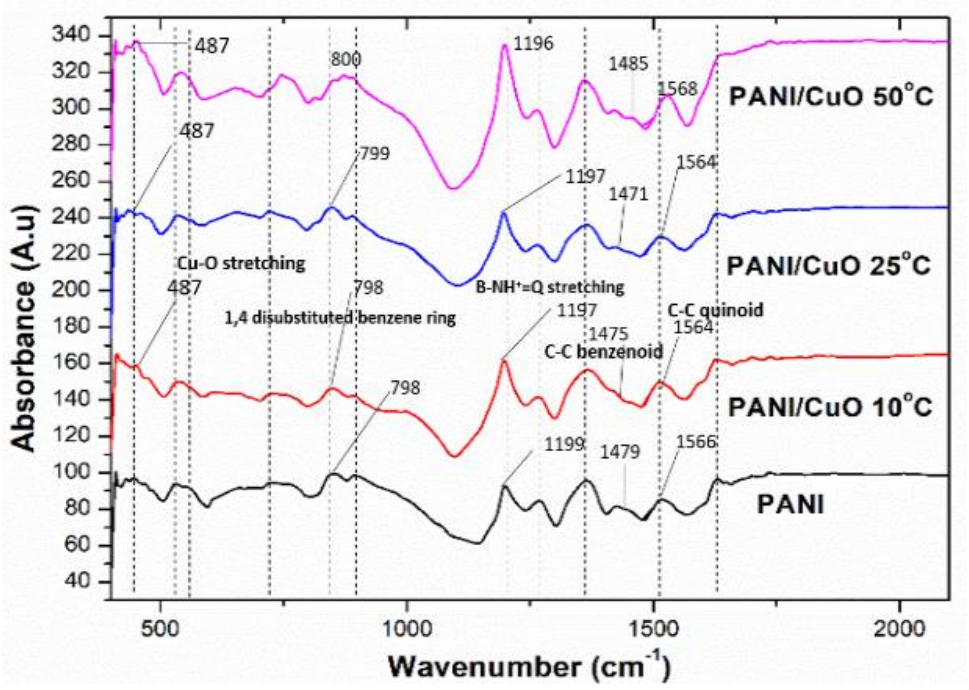

Figure 7. FTIR spectrum of PANI and PANI/CuO nanocomposites at wavelength 400-2100 nm.

In its emeraldine salt form, PANI exhibits a greenish colour; it is characterised by these specific peaks, indicating that the material is half-oxidized and electrically conductive [25]. The FTIR spectra in Figure 7 confirm the emeraldine salt form of PANI by

the presence of the quinoid ring (Q) and benzenoid ring (B) vibrational peaks at 1556 cm^{-1} and 1479 cm^{-1}, respectively, for pure PANI. The data also show that the peak intensity ratio of the Q and B ring vibrational modes (I_Q/I_B) is nearly equal, which is typical for synthesised PANI ES samples. A different behaviour was observed in the case of PANI/CuO nanocomposites. The spectra exhibited overlapping peaks for the quinoid and benzenoid rings, resulting in a single broad peak with a blue shift at wave numbers 1475.54 cm^{-1} and 1471 cm^{-1} for the PANI/CuO nanocomposites synthesised at 10℃ and 25℃, respectively. For the PANI/CuO nanocomposite synthesised at 50℃, a red shift occurred with the quinoid ring peak appearing at 1485 cm^{-1} compared to pure PANI. These peak shifts suggest changes in the electronic structure of the composites, indicating possible interactions between PANI and CuO. These interactions may enhance electron delocalisation within the polymer matrix, potentially improving the electrical conductivity of the nanocomposites [25].

The peak intensity ratio of Q and B rings vibrational modes (I_Q/I_B) in PANI/CuO nanocomposites deviates from that of pure PANI, indicating that the synthesised PANI/CuO nanocomposites are not in a half-oxidized state [25]. The presence of CuO and the effects of higher synthesis temperatures significantly influence the characteristics of PANI/CuO nanocomposites. Specifically, adding CuO enhances electrical conductivity and thermal stability due to improved electron transfer and heat dissipation facilitated by the metal oxide. Higher synthesis temperatures promote better dispersion of CuO nanoparticles within the PANI matrix, leading to a more uniform polymerisation process. The observed shifts in the FTIR spectra can be attributed to hydrogen bonding between the NH group of PANI and the Cu–O on the CuO particle surface. This hydrogen bonding enhances the interaction between the polymer matrix and the metal oxide nanoparticles, leading to improved dispersion and stronger interfacial adhesion. These interactions contribute to the overall structural integrity of the nanocomposites, improving their electrical conductivity and thermal stability [17].

The peaks at 487 cm^{-1} and 586 cm^{-1} correspond to the characteristic stretching vibrations of the Cu–O bond [17]. The incorporation of CuO into PANI is known to improve the thermal stability of the resulting nanocomposites [17]. The main characteristic frequencies of PANI and PANI/CuO nanocomposites, including wave numbers and vibrational modes, are summarised in Table 1.

The FTIR spectra also reveal new peaks at 1038, 1211, and 1410 cm^{-1} in the high-temperature synthesis of PANI/CuO nanocomposites, which are not present in pure PANI synthesised at 273 K. The peak at 1038 cm^{-1} is attributed to the vibrational modes of the phenazine structure. The peak at 1211 cm^{-1} corresponds to the stretching mode of C–N or the bending mode of C–H in 1,4-disubstituted structures, indicating the formation of the phenazine structure. Meanwhile, the peak at 1410 cm^{-1} represents a combination of vibrational modes from

phenazine, safranine, and phenoxazine [11, 25]. The phenazine structure is formed due to the rapid polymerisation process under high-temperature conditions, where anilinium ions create bonds with imine groups at the ortho position, forming the phenazine structure [25]. The formation of phenazine, phenoxazine, and safranine in PANI/CuO nanocomposites generally tends to decrease the electrical conductivity of the composite [11].

A peak at 2372–2374 cm^{-1} represents the stretching vibrations due to a substituent methyl group [17], as shown in Figure 8. The broad peak at 3200–3400 cm^{-1} is attributed to O–H stretching in both PANI and PANI/CuO nanocomposites, which occurs due to H_2O content in the materials.

Table 1. Characteristic frequencies of PANI and PANI/CuO nanocomposites

PANI	PANI/CuO 10° C	PANI/CuO 25° C	PANI/CuO 50° C	Vibration Mode
	Wavenumber (cm^{-1})			
3300.51	3294.86	3290.15	3280.28	O-H stretching
3172.90	2922.16	3153.61	3190.26	C-H stretching
2372.44	2372.44	2372.44	2372.44	Stretching due to substituent methyl group
1658.78	1658.78	1658.78	1658.78	C-H bending C=N stretching
1566.20	1564.27	1564.27	1568.13	C=C quinoid
1479.40	1475.54	1471.69	1485.19	C-C benzenoid
1406.11	1407	1409.96	1408.04	Phenazine; Safranine phenoxazine
1301.95	1300.02	1300.02	1300.02	C-N secondary aromatic amine
1242.16	1242.16	1240.23	1244.09	$C\text{-}N^+$
1199.79	1197	1197	1196	$B\text{-}NH^+\text{=}Q$
1095	1097.50	1103.28	1093.64	C-N stretching
879.54	878	877.61	876.2	C-H stretching
798.39	798.46	799.60	800.46	1,4 disubstitute benzene ring
	586.36	588.29	587.25	Inorganic group
-	437	437	437	Cu-O inorganic group

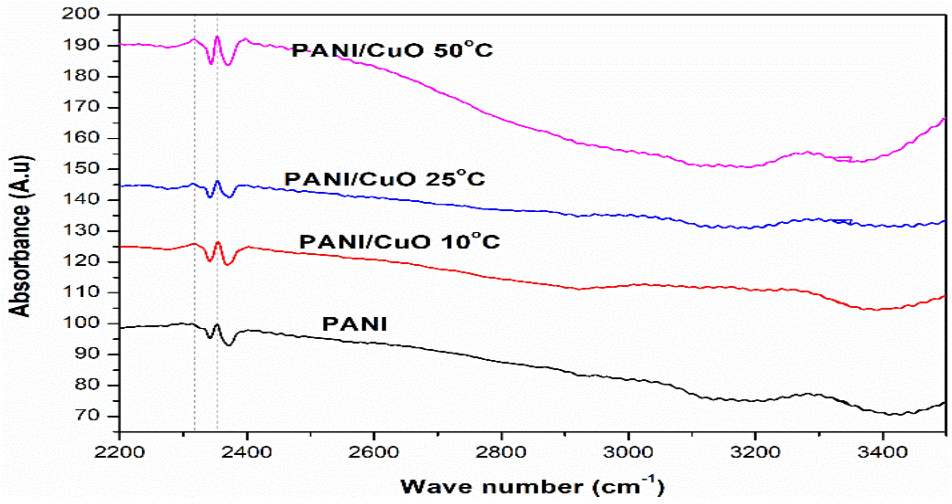

Figure 8. FTIR spectrum of PANI and PANI/CuO nanocomposites at wavelength 2200-3400 nm

3. Morphological Analysis of PANI and PANI/CuO Nanocomposites

The SEM micrograph of pure PANI (Figure 9) exhibits a uniform globular morphology [25]. In contrast, the PANI/CuO nanocomposite synthesised at 50°C (Figure 10) shows a nanorod morphology, although the CuO particles are not evenly distributed. The formation of nanorods is typically associated with high synthesis temperatures, which accelerate the polymerisation of aniline [25].

These morphological differences significantly impact the material's properties and potential applications. The globular morphology of pure PANI generally results in a lower surface area, which may limit its conductivity and effectiveness in certain applications. Conversely, the nanorod morphology observed in the PANI/CuO nanocomposite increases the surface area, thereby enhancing electron transport pathways and improving electrical conductivity [11, 25]. This increased surface area also enhances the effectiveness of the nanocomposite in applications such as sensors, catalysis, and energy storage, where high surface interaction is essential for optimal performance.

The presence of hydrogen bonding between the NH group of PANI and CuO on the surface of CuO particles, as depicted in Figure 11, can accelerate charge transfer between PANI and CuO. This enhanced charge transfer makes PANI/CuO nanocomposites particularly suitable for electronic materials, such as energy storage devices and solar cells.

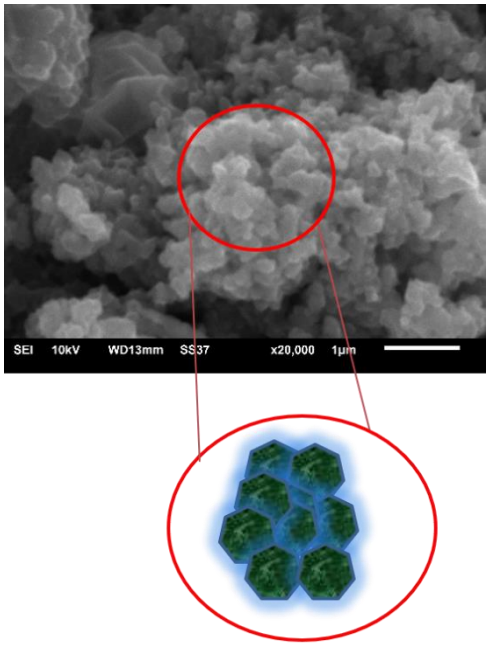

Figure 9. SEM micrograph profile of pure PANI

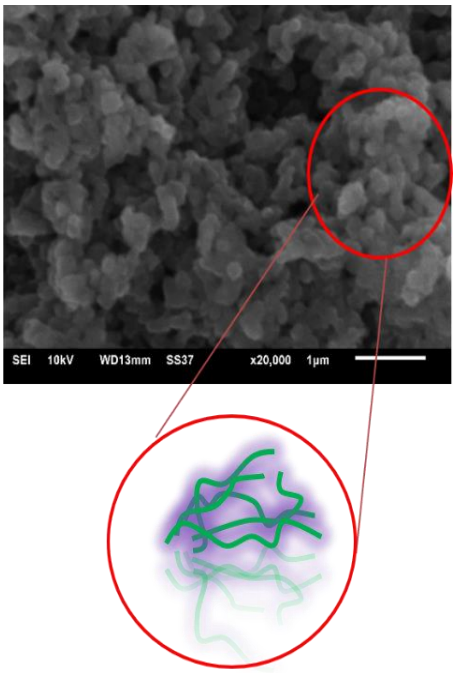

Figure 10. SEM micrograph profile of PANI/CuO 50℃ nanocomposites

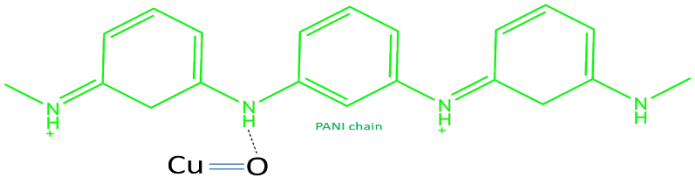

Figure 11. Schematic of Hydrogen bonding between NH group of PANI and Cu-O on the surface of CuO particles

CONCLUSION

This study aimed to synthesise and characterise PANI/CuO nanocomposites under different synthesis temperature conditions. PANI/CuO nanocomposites were successfully synthesised at 10°C, 25°C, and 50°C. The FTIR spectra of PANI and PANI/CuO nanocomposites revealed distinct features, particularly in the quinoid and benzenoid ring regions, with shifts observed at wave numbers 1475.54 cm^{-1} and 1471 cm^{-1} for the PANI/CuO nanocomposites synthesised at 10°C and 25°C, respectively. In contrast, the PANI/CuO nanocomposite synthesised at 50°C exhibited a quinoid ring peak at 1485 cm^{-1}. These shifts are attributed to the formation of hydrogen bonds between the NH group of PANI and the Cu-O bonds on the surface of CuO particles. SEM micrographs revealed that pure PANI exhibits a uniform globular morphology, whereas the PANI/CuO nanocomposites display a nanorod morphology.

.

ACKNOWLEDGEMENT

acknowledges to LPPM UIN Sunan Gunung Djati Bandung for funding this research in litapdimas program, ministry of religious affair 2024.

REFERENCES

[1] K. Lata and R. K. Rana, "Synthesis and characterization of polyaniline-copper oxide nano-composites," *Int J Chem Stud*, vol. 12, no. 1, pp. 46–50, Jan. 2024, doi:10.22271/chemi.2024.v12.i1a.12396.

[2] Asha et.al., "Synthesis and characterization of polyaniline/TiO_2 composites," *Indian journal of pure and app Physics*, vol. 52, pp. 341-347, May 2014.

[3] F. R. Rangel-Olivares et.al., "Synthesis and characterization of polyaniline-based polymer nanocomposites as anti-corrosion coatings," *Coatings*, vol. 11, no. 6, Jun. 2021, doi: 10.3390/coatings11060653.

[4] S. L. Goyal et.al., "Synthesis and characterization of polyaniline/TiO_2 composites," *Indian journal of pure and app Physics*, vol. 52, pp. 341-347, May 2014.

[5] A. Mostafaei and A. Zolriasatein, "Synthesis and characterization of conducting polyaniline nanocomposites containing ZnO nanorods," *Progress in Natural Science: Materials International*, vol. 22, no. 4, pp. 273–280, Aug. 2012, doi: 10.1016/j.pnsc.2012.07.002.

[6] L. Yesappa et.al., "Characterization, Electrical Conductivity and Electrochemical Performance of Polyaniline-$LiClO_4$-CuO Nano Composite for Energy Storage Applications," *Polymer-Plastics Technology and Materials*, vol. 58, no. 2, pp. 193–205, Jan. 2019, doi:10.1080/03602559.2018.1466175.

[7] N. Boutaleb et.al., "Facile Synthesis and Electrochemical Characterization of Polyaniline@TiO_2-CuO Ternary Composite as Electrodes for Supercapacitor Applications," *Polymers (Basel)*, vol. 14, no. 21, Nov. 2022, doi: 10.3390/polym14214562.

[8] D. Doğan et.al., "Increasing Photocatalytic Stability and Photocatalytic Property of Polyaniline Conductive Polymer," *Iran J Sci Technol Trans A Sci*, vol. 44, no. 4, pp. 1025–1037, Aug. 2020, doi: 10.1007/s40995-020-00922-3.

[9] R. R. Sunarya et.al., "Combination of polyaniline and graphene oxide as counter electrode composites in dye-sensitized solar cells," in *AIP Conference Proceedings*, American Institute of Physics Inc., Apr. 2023. doi: 10.1063/5.0115886.

[10] A. I. Fatya et.al., "Synthesis of polyaniline/electrochemically exfoliated graphene composite as counter-electrode in dye-sensitized solar cell," *Polymer-Plastics Technology and Materials*, vol. 59, no. 12, pp. 1370–1378, Aug. 2020, doi:10.1080/25740881.2020.1738479.

[11] R. R. Sunarya et.al., "Electrocatalytic Activation of a DSSC Graphite Composite Counter Electrode Using In Situ Polymerization of Aniline in a Water/Ethanol Dispersion of Reduced Graphene Oxide," *J Electron Mater*, vol. 49, no. 5, pp. 3182–3190, May 2020, doi: 10.1007/s11664-020-07977-3.

[12] N. Fauziah et.al., "Ultrasonication-modified electrochemically exfoliated graphene for counter electrode in dye-sensitized solar cells," *Carbon Trends*, vol. 12, Sep. 2023, doi: 10.1016/j.cartre.2023.100292.

[13] R. Rahmawati et.al., "Reduced Graphene Oxide/Polyaniline Nanocomposite as Efficient Counter Electrode for Dye Sensitized Solar Cells," in *IOP Conference Series: Materials Science and Engineering*, Institute of Physics Publishing, Jul. 2018. doi:10.1088/1757899X/384/1/012040.

[14] H. Meskher et.al., "Synthesis and Characterization of CuO@PANI composite: A new prospective material for electrochemical sensing," *Journal of Composites and Compounds*, vol. 4, no. 13, pp. 178–181, Dec. 2022, doi: 10.52547/jcc.4.4.1.

[15] M. Nagaraja et.al, "Polyaniline-CuO nanocomposite: Electrical, structural and sensor properties," in *Materials Today: Proceedings*, Elsevier Ltd, 2021, pp. 1989–1992. doi: 10.1016/j.matpr.2021.08.154.

[16] L. G. Yesappa et.al., "Structure, morphology and optical properties of CuO nano particles immersed PANI/Li composite," in *AIP Conference Proceedings*, American Institute of Physics Inc., Jun. 2020. doi: 10.1063/5.0009090.

[17] S. Ashokan et.al., "Synthesis and characterization of CuO nanoparticles, DBSA doped PANI and PANI/DBSA/CuO hybrid composites for diode and solar cell device development," *J Alloys Compd*, vol. 646, pp. 40–48, Jun. 2015, doi: 10.1016/j.jallcom.2015.05.088.

[18] X. M. He et.al., "Facile synthesis of polyaniline-coated SiO_2 nanofiber and its application in enrichment of fluoroquinolones from honey samples," *Talanta*, vol. 140, pp. 29–35, Aug. 2015, doi: 10.1016/j.talanta.2015.03.006.

[19] S. Islam et.al., "Synthesis, electrical conductivity, and dielectric behavior of polyaniline/V_2O_5 composites," *Int J Polym Sci*, vol. 2013, 2013, doi: 10.1155/2013/307525.

[20] R. Li et.al., "Intercalated polyaniline in V_2O_5 as a unique vanadium oxide bronze cathode for highly stable aqueous zinc ion battery," *Energy Storage Mater*, vol. 38, pp. 590–598, Jun. 2021, doi: 10.1016/j.ensm.2021.04.004.

[21] Z. A. Boeva and V. G. Sergeyev, "Polyaniline: Synthesis, properties, and application," *Polymer Science - Series C*, vol. 56, no. 1, pp. 144–153, 2014, doi: 10.1134/S1811238214010032.

[22] V. Babel and B. L. Hiran, "A review on polyaniline composites: Synthesis, characterization, and applications," Jul. 01, 2021, *John Wiley and Sons Inc*. doi: 10.1002/pc.26048.

[23] F. Fenniche et.al., "Synthesis and characterization of PANI nanofibers high-performance thin films via electrochemical methods," *Results Chem*, vol. 4, Jan. 2022, doi: 10.1016/j.rechem.2022.100596.

[24] M. Reza et.al., "Variation of Ammonium Persulfate Concentration Determines Particle Morphology and Electrical Conductivity in HCl Doped Polyaniline," in *IOP Conference Series: Materials Science and Engineering*, Institute of Physics Publishing, Sep. 2019. doi:10.1088/1757899X/599/1/012002.

[25] A. N. Amalina et.al., "Preparation of polyaniline emeraldine salt for conducting-polymer-activated counter electrode in Dye Sensitized Solar Cell (DSSC) using rapid-mixing polymerization at various temperature," *Bulletin of Chemical Reaction Engineering and Catalysis*, vol. 14, no. 3, p. 521, 2019, doi: 10.9767/bcrec.14.3.3854.521-528.

[26] Q. Zhang et.al., "CuO nanostructures: Synthesis, characterization, growth mechanisms, fundamental properties, and applications," 2014, *Elsevier Ltd*. doi: 10.1016/j.pmatsci.2013.09.003.

[27] S. Raja and M. Deepa, "Synthesis and characterization of polyaniline-copper (II) oxide nanocomposite by wet chemical route," *Indian Journal of*

Advanced Chemical Science, vol. 3, pp. 198–203, 2015.

[28] L. I. Nadaf and K. S. Venkatesh, “Polyaniline-Copper Oxide Nano-Composites: Synthesis and Characterization,” *Material Science Research India*, vol. 12, no. 2, pp. 108–111, Dec. 2015, doi: 10.13005/msri/120204.

[29] D. Manyasree et.al., “CuO nanoparticles: Synthesis, characterisation and their bactericidal efficacy,” *International Journal of Applied Pharmaceutics*, vol. 9, no. 6, pp. 71–74, Oct. 2017, doi: 10.22159/ijap.2017v9i6.71757.

[30] W. Sun et.al., “Hierarchically porous hybrids of polyaniline nanoparticles anchored on reduced graphene oxide sheets as counter electrodes for dye-sensitized solar cells,” *J Mater Chem A Mater*, vol. 1, no. 8, pp. 2762–2768, Feb. 2013, doi: 10.1039/c2ta01000c.

[31] K. A. Ibrahim, “Synthesis and characterization of polyaniline and poly(aniline-co-o-nitroaniline) using vibrational spectroscopy,” *Arabian Journal of Chemistry*, vol. 10, pp. S2668–S2674, May 2017, doi: 10.1016/j.arabjc.2013.10.010.

[32] Y. Kovalyshyn et.al., “Synthesis and Electrochemical Properties of Polyaniline Composites,” in *Proceedings of the 2020 IEEE 10th International Conference on “Nanomaterials: Applications and Properties”, NAP 2020*, Institute of Electrical and Electronics Engineers Inc., Nov. 2020. doi:10.1109/NAP51477.2020.9309531.